CHAPTER 3

ASSESSMENT OF HORIZONTAL DUST FLUX LOADING OVER SISTAN

3.1 Introduction

Dust storms, as the most important source of mineral aerosols in the atmosphere, frequently occur in arid and semi-arid regions of the world, Dust storms are regarded as a serious environmental hazard (Prospero *et al.*, 2002). Each year, several billion tons of soil-dust is entrained into the atmosphere, playing a vital role in solar irradiance attenuation, and affects marine environments, atmospheric dynamics and even weather (Tegen and Fung, 1994, Tegen *et al.*, 1996; Dunion and Velden, 2004; Prasad *et al.*, 2007; Singh *et al.*, 2008; Patadia *et al.*, 2009).

Desert dust is considered to be a major component of tropospheric aerosols over the globe (Mishchenko and Geogdzhayev, 2007) with global flux estimations of 1500 to 2600 $Tg.yr^{-1}$ (IPCC, 2007). Estimates of dust emissions from the Sahara desert range from 130 to 760 Tg yr^{-1} (Goudie and Middleton, 2001), while another study (Ozer, 2001) estimated the annual Saharan dust emissions to be about 1600 Tg yr^{-1}. For comparison purposes the global dust emissions range from 1000 to 3000 Tg yr^{-1} (Zender *et al.*, 2004). On an annual basis, about 80 to 120 Tg of dust are transported to the Mediterranean area south of Europe (d' Almeida, 1986). Barnaba and Gobbi (2004) found a total seasonal mean value of 119 ktons of desert dust per day to be injected into the Mediterranean atmosphere, corresponding to a total of 4.3×10^4 ktons of dust in 2001. Anthropogenic sources were previously considered as important dust contributors (IPCC, 2001), but more recently (IPCC, 2007) were estimated to contribute only 5 to 7% of total mineral dust. The impact of dust aerosols in the Earth's system depends mainly on particle characteristics such as size, shape and mineralogy (Mahowald *et al.*, 2005), which are initially determined by the terrestrial sources from which the soil sediments are entrained and from their chemical composition (Claquin *et al.*, 1998). On the other hand, particle size distributions provide fundamental information for rock characterization and geological process, including

sedimentology, stratigraphy, structural geology, pedology and volcanology (e.g. Kandler *et al.*, 2009). Although, during recent years, satellite remote sensing of dust has been increasingly available with promising and reliable results, in-situ measurements for dust aerosol characteristics and dust loading are still considered absolutely essential. For this reason, several campaigns have been conducted in the arid areas of the globe, mainly focusing on the Sahara as the largest and most active dust source region. Although the dust activity and plume exposures from the Sahara to both the Atlantic and Mediterranean Oceans have been extensively investigated over the years, significantly fewer studies have been conducted over the Middle East and southwest Asia.

This Chapter aims at defining the Hamoun basin as a major dust source region by focusing on the assessment of dust loading at two nearby locations. The experimental campaign took place from August 2009 to July 2010, a period when the dust loading at different altitudes during major dust events from the Hamoun basin were measured. The grain size is used to provide useful information regarding the status of Sistan's dust storms. Such studies are currently lacking in this region, and the work in this thesis is the very first that examines the evolution of dust sediments over the Sistan arid environment.

3.2 Horizontal dust flux loading measurements

The measurement of amounts of dust flux is one of the most problematic procedures in dust studies. Airborne dust concentration, for example, is usually calculated from horizontal flux data. Also, the rate of deposition of particles on the surface is a direct function of both the vertical and the horizontal dust flux. Vertical dust flux samplers have been extensively described in literature (Clements *et al.*, 1963; Köhler and Fleck, 1963; Clough, 1975; Ganor, 1975; Ralph and Barrett, 1976; Skärby, 1977; Goodman *et al.*, 1979; Bücher, 1986; Hall and Waters, 1986; Hall and Upton, 1988; Goossens and Offer, 1990; Orange *et al.*, 1990; Pye, 1992; Offer *et al.*, 1992; Goossens and Offer, 1993; Littmann, 1997). Vertical samplers are usually passive, i.e., the air is not actively sucked into the trap.

On the other hand, horizontal dust flux samplers have been described by Steen (1977), Wilson and Cooke (1980), White (1982), Fryrear, (1986), Ralph and Hall, (1989), Stout and Fryrear (1989), Janssen and Tetzlaff, (1991), Leys and Raupach, (1991),

Nickling and Gillies (1993), Shao *et al.* (1993) and Hall *et al.*, (1994). These are all passive devices, except for the samplers used by Nickling and Gillies, (1993) and Leys and Raupach, (1991), which use pumping to maintain airflow through a trap.

3.3 Description of the dust samplers

3.3.1 Big Spring Number Eight (BSNE) sampler

The Big Spring Number Eight (BSNE) sampler was developed by Fryrear, (1986). Although it was originally designed to collect airborne dust, it is now also frequently used to collect soil and sand. A picture and a technical diagram is shown in Fig. 3.1. Dust-laden air passes through a vertical 2 cm×5 cm sampler opening. Once inside the sampler, air speed is reduced and the dust settles in a collection pan. Air discharges through a 60-mesh screen. An 18-mesh screen reduces the movement of the deposited material, preventing breakdown of the collected sediment and potential loss of very fine particles out of the top of the screen. A rubber retainer closes any small holes in the back or front of the assembled sampler. A wind vane at the rear insures the sampler is turned to the wind. More details about the sampler can be found in the original description by Fryrear, (1986).

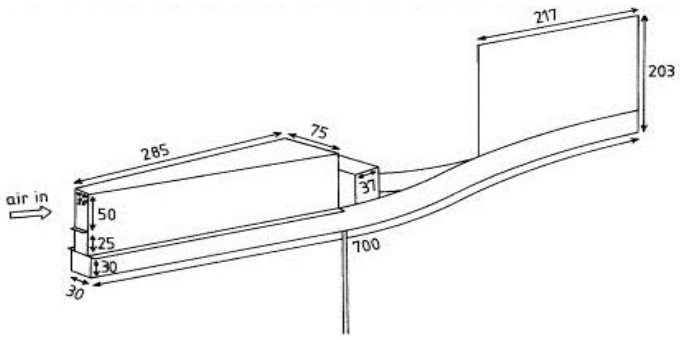

Figure 3.1: Construction of the Big Spring Number Eight (BSNE) sampler. Dimensions are in mm

3.3.2 SUspended Sediment TRAp (SUSTRA) sampler

The SUspended Sediment TRAp (SUSTRA) was developed by Janssen and Tetzlaff, (1991). Similar to the BSNE, it is now used for the collection of different types of sediment (dust, sand and soil). A picture and a technical diagram is shown in Fig. 3.2. The dust-laden air enters the instrument via a horizontal metal tube 5 cm in diameter and rebounds onto a metal plate inside a central vertical pipe. Particles settle onto a plastic dish

placed on top of an electronic balance underneath the pipe, except the finest ones, which may leave the sampler via a small outlet on top of the pipe (together with the air discharging from the instrument). Similar to the BSNE, a wind vane turns the instrument into the wind at all times. To minimise airflow disturbance near the surface, the balance is placed in a metal box dug into the ground. In the original version the horizontal inlet tube is at a height of about 23 cm above the surface, but this value can be adjusted while digging the balance box into the ground. More details on the instrument are described in the original paper by Janssen and Tetzlaff, (1991).

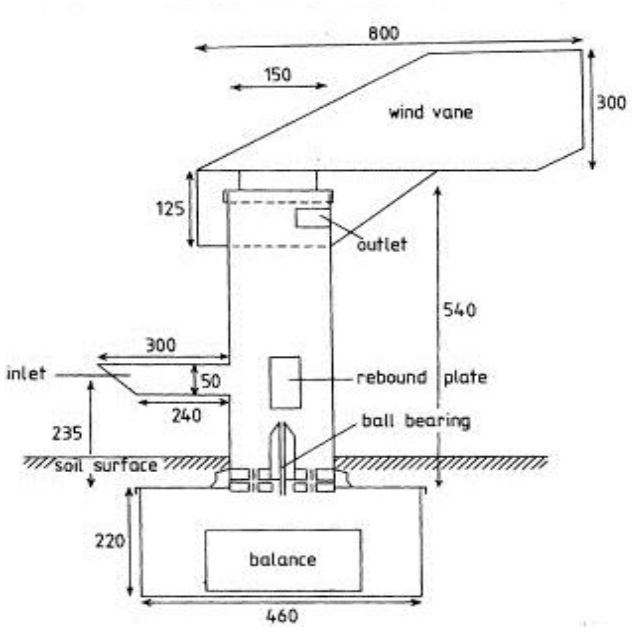

Figure 3.2: Construction of the SUspended Sediment TRAp (SUSTRA) sampler. Dimensions are in mm

3.3.3 Modified Wilson and Cooke (MWAC) sampler

The Modified Wilson and Cooke (MWAC) sampler is based on an original design developed by Wilson and Cooke, (1980). The sampler consists of a plastic bottle, figuring as settling chamber, to which an inlet tube and an outlet tube have been added (Fig. 3.3). The bottle is installed vertically, with the inlet oriented to the wind. Sediment entering the bottle will be deposited due to the pressure drop created by the difference in diameter between the bottle and the inlet and outlet tubes. The clean air then discharges from the bottle via the outlet.

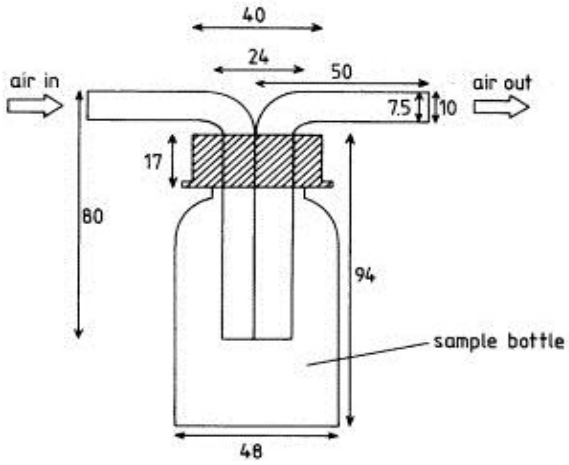

Figure 3.3: Sketch and construction of the Modified Wilson and Cooke (MWAC) sampler. Dimensions is in mm

The original concept was later slightly modified by Kuntze *et al.*, (1990), who attached the bottle in a horizontal (not vertical) position to a mast provided with a wind vane. By attaching several bottles at different levels to the mast, vertical flux profiles can be measured (Sterk, 1993).

3.3.4 Wedge Dust Flux Gauge (WDFG) sampler

The Wedge Dust Flux Gauge (WDFG) was developed by Hall *et al.*, (1994). A picture and a technical diagram is shown in Fig. 3.4. The WDFG consists of a simple, parallel sided box, wedge shaped in elevation and with extended sides towards the rear holding a baffle plate. The flat, horizontal bottom of the box is 18 cm long and 10 cm wide.

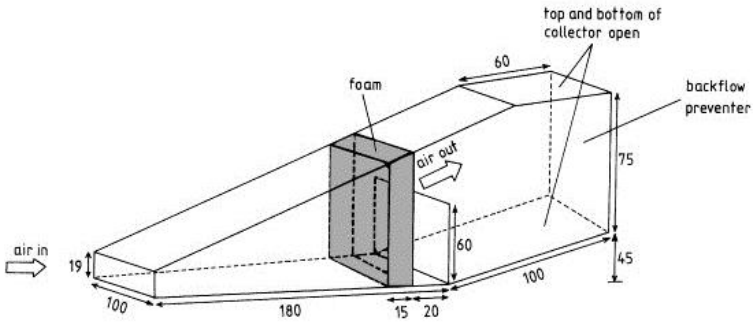

Figure 3.4: Sketch and construction scheme of the Wedge Dust Flux Gauge (WDFG) sampler. Dimensions is in mm

The top slopes upwards at an angle of 24.5°. Sediment-laden air enters the instrument via a 1.9×10.0 cm rectangular slot. The box contains a particle trap made from

10 pores in^{-1} open-celled foam, which is normally sprayed with a thin sticky coating to retain any impacting particle. More details about the WDFG can be found in the original description by Hall *et al*. (1994).

3.3.5 Siphon Sand and Dust Sampler (SSDS) sampler

The Siphon Sand and Dust Sampler (SSDS) was developed by Ekhtesasi (2003), which he later slightly modified (Ekhtesasi *et al*., 2009). The sampler consists of a tube with a diameter of 9 cm. The sediment-laden air passes through a vertical 4 cm x 6 cm sampler opening in the middle. Inside the sampler, air speed is reduced and the particles settle in a collection pan at the bottom, while the air discharges through an outlet with a U shape.

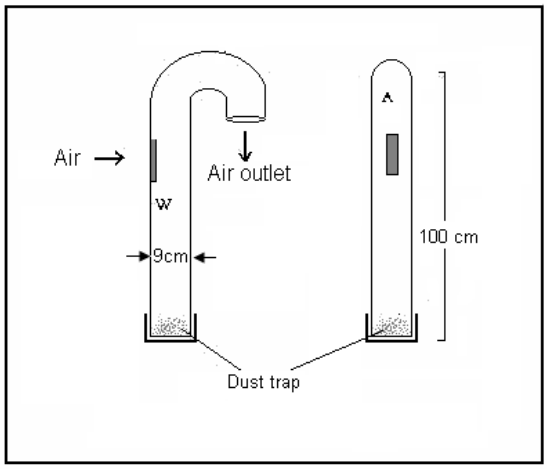

Figure 3.5: Construction of the Siphon Sand and Dust Sampler (SSDS) sampler

3.4 Particle-size analysis

Particle-size distribution is a key parameter determining the entire process of dust storms and wind erosion, from entrainment through transport to deposition. It can be estimated from either a geometric or the dynamic point of view. From the geometric perspective, particle-size distributions can be determined using one of three methods: (a) dry or wet sieving; (b) electro-optical techniques, including Coulter Counter analysis and laser granulometry, and (c) computerised image analysis. From the dynamic perspective, the distribution of the particle terminal velocity can be measured using a settling tube or an elutriator. The choice of the most appropriate method depends largely on the amount of fine material present in the soil sample and the intended applications of the data set.

Samples which contain only small amounts of fine material can be analysed through dry-sieving or settling-tube analysis, whereas Coulter-Counter analysis or laser granulometry are more adequate if the sample contains a significant quantity of dust particles. Image analysis can be employed if both size and shape information is needed.

3.4.1 Dry sieving

Dry sieving is undertaken using a stack of successively-finer sieves, which are mounted on an electrically-powered shaker (Pye and Tsoar, 1990). The shakers have simple vibrating, rotating and tilting actions or have a hammer action. Each sieve consists of a stainless-steel, brass, phosphor-bronze or nylon mesh. The optimum size used for dry sieving depends on the number of sieves and the dimensions of the mesh aperture. Standard permissible sieve-loading according to the British Standards Institution is given in Table 3.1.

Table 3.1: Recommended sieve aperture and maximum permissible sieve loading

Mesh(mm)	20	14	10	6.3	5	3.35	2.0
Load(Kg)	2.0	1.5	1.0	0.75	0.5	0.3	0.2
Mesh(mm)	1.18	0.6	0.425	0.3	0.212	0.15	0.063
Load(Kg)	0.1	0.075	0.075	0.05	0.05	0.04	0.025

3.4.2 Electro-Sensing Methods

One of the instruments used for particle-size analysis is the Coulter Multisizer. The instrument is best suited for handling small samples with a narrow particle-size range. For such samples, the time required for the analysis is short, the resolution is very high, and the reproducibility is good. The Multisizer is less well-suited to samples with a broad particle-size range.

The Coulter Multisizer is based on the Coulter principle (Fig. 3.6). The number and size of particles are measured by suspending the sample in a conductive liquid and measuring the electrical current between two electrodes on either side of a small aperture, through which particles are sucked. As each particle passes through the sensing zone and aperture it changes the impedance of the current between the two electrodes, producing a pulse with a magnitude proportional to the particle volume. These current pulses are

scaled, counted and accumulated in 256 size-related channels from which a particle-size distribution is produced. The Coulter Multisizer produces size distributions in terms of volume, number and particle surface area.

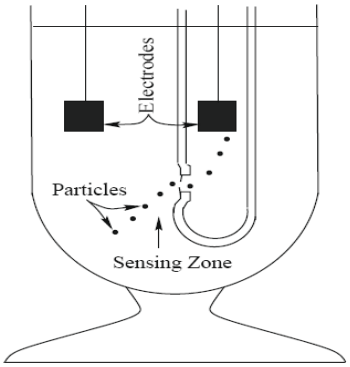

Figure 3.6: Illustration of the electrical sensing zone, showing an aperture tube immersed in an electrolyte with particles passing through the aperture (Redrawn from McTainsh *et al.*, 1997)

The nature of sample pre-treatment has a significant effect on the results of the analyses. As the sample must be analysed in a liquid electrolyte [3% tri-sodium orthophosphate (Na_3PO_412H2O) plus 50% glycerol], the Coulter Multisizer cannot perform undispersed particle-size analyses, i.e., the analyses are always more or less dispersed. If the analysis is done without intentionally dispersing the sample through additional chemical or physical treatments, it is called minimally-dispersed and the resultant particle-size distribution is referred to as the minimally-dispersed particle-size distribution. For most soils, this is probably not too different from the in-situ particle-size distribution or the best approximation to it currently available. For the fully-dispersed analysis, the soil sample receives chemical and vigorous physical dispersions to reduce it to its fundamental particle-size constituents. A typical chemical treatment is to place the sample in a soil dispersant, such as 3% tri-sodium orthophosphate and 1M sodium hydroxide (NaOH). The particle-size analysis of the soil sample after the chemical and physical treatments gives the fully-dispersed particle-size distribution. This particle-size distribution is the best approximation available for that of the sediment during a very strong wind-erosion event. In wind-erosion modelling, the fully-dispersed particle-size analysis is used to estimate the mass fraction of dust in a given soil (Shao, 2010).

One of the advantages of the Coulter Multisizer is its capacity to analyze samples in very small quantities down to about 0.1 g, while other particle-size analysis techniques, such as hydrometer and sieve analyses, require samples up to 30 g. This feature of the

Coulter Multisizer allows the particle-size analysis of sediment samples collected using high-volume samplers. The Coulter Multisizer also produces a relatively-high resolution for particle-size analysis, since particles are sized into 256 classes. The multisizer can measure particles over a size range from 0.45 to 1200µm, but there are practical difficulties with analyses at the coarse end (>150 µm), and the Multisizer appears to underestimate the clay fraction (<2 µm) (McTainsh *et al*., 1997). For the <2 µm fraction, pipette analysis can be performed instead.

3.4.3 Laser granulometry

Laser granulometry is based on the principle that there is a direct relationship between the size of particles and the degree to which they diffract light. In the case of the Malvern Instruments Laser Particle Sizer Type 3600E, a beam of monochromatic light (wave length 633 nm) is passed through a cell containing the sample in suspension and the diffracted light is focused onto a detector which senses the angular distribution of scattered light energy (McCave *et al*., 1986). The size range detected depends on the focal length of the focusing lens, which is placed between the sample cell and the detector. Grains are kept in suspension by a mechanical stirring device. Three lenses are available, each of which divides the distribution into 15 size classes. The 300 mm focal length lens has a range of 5.8 to 560 µm and is therefore most appropriate for sands. However, the coarsest of the 15 class intervals have a very wide range (261 to 264 µm).

3.4.4 Abrasion emitter

The dust-emission potential of a given soil is the mass fraction of dust particles that can be released during the process of wind erosion. It is a key quantity to be determined for dust-emission modelling. This potential is related to the observation that different techniques for particle-size analysis produce different particle-size distributions, depending on the degree of the mechanical and/or chemical destructions applied to the soil sample. To approximate dust-emission potential, Lu and Shao (1999) introduced the concept of minimally-disturbed and fully-disturbed particle-size distributions. However, it is not exactly clear what laboratory methods should be used to determine these two particle-size distributions. Shao (2001) assumed that they can be approximated, respectively by using the minimally-dispersed particle size distribution and fully-dispersed particle-size distribution. This assumption now appears to be questionable, because

evidence suggests that the effect of saltation bombardment, even under strong wind conditions, is likely to be much weaker than that of chemical treatment in the laboratory (Fig. 3.7b).

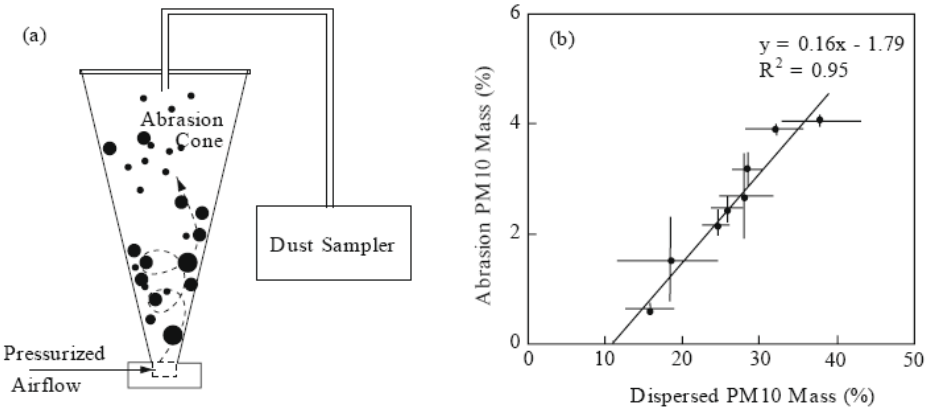

Figure 3.7: (a) A schematic illustration of an abrasion emitter; (b) Emission potential for PM10 for 8 soils plotted against the corresponding PM10 mass fractions determined using a dispersed analysis technique (Redrawn from Chandler *et al*., 2002)

Chandler *et al*. (2002) designed a laboratory technique for measuring dust-emission potential. This technique deserves particular attention. The instrument they used couples an abrasion emitter with a dust sampler, e.g. a Tapered Element Oscillating Microbalance or an Optical Particle Counter (Fig. 3.7a). The abrasion emitter is a stainless steel cone attached to a pressurised airflow which can be regulated. The soil sample is placed in a cup located close to the base of the cone. The top of the cone is closed with a plate, and a tube is inserted through the plate to aspirate air from the cone for monitoring dust emission. The pressured airflow fluidizes the soil sample in the cup and propels the particles upward in a rotating motion inside the cone. Abrasion takes place as the particles tumble and slide along the interior surface of the cone. The dust-emission potential of the tested soil is then determined as the ratio of the mass collected by the dust sampler over a run (about one hour) to the mass of the soil sample (Shao, 2010).

3.5 Data set and experimental methods

3.5.1 Dust loading measurements and mass quantities

The amount of dust loadings during dust storms was measured using passive dust samplers (Fig.3.9a) fixed at two monitoring towers (respectively, at four and eight meters above ground level in altitude), with one meter distance between the adjacent individual traps. The four meters tower had four traps and the eight meters tower had eight traps (Fig. 3.9b). The measurements were done during the period August 2009 to July 2010. The towers were erected at two open locations near Hamoun (31.08^{o}N, 61.54^{o}E and 31.26^{o} N, 61.76^{o}E), which are sufficiently distant from any obstacles which ensured that undisturbed wind flow could enter for taking representative dust samples (station A and station B, denoted by red stars in Fig. 3.8).

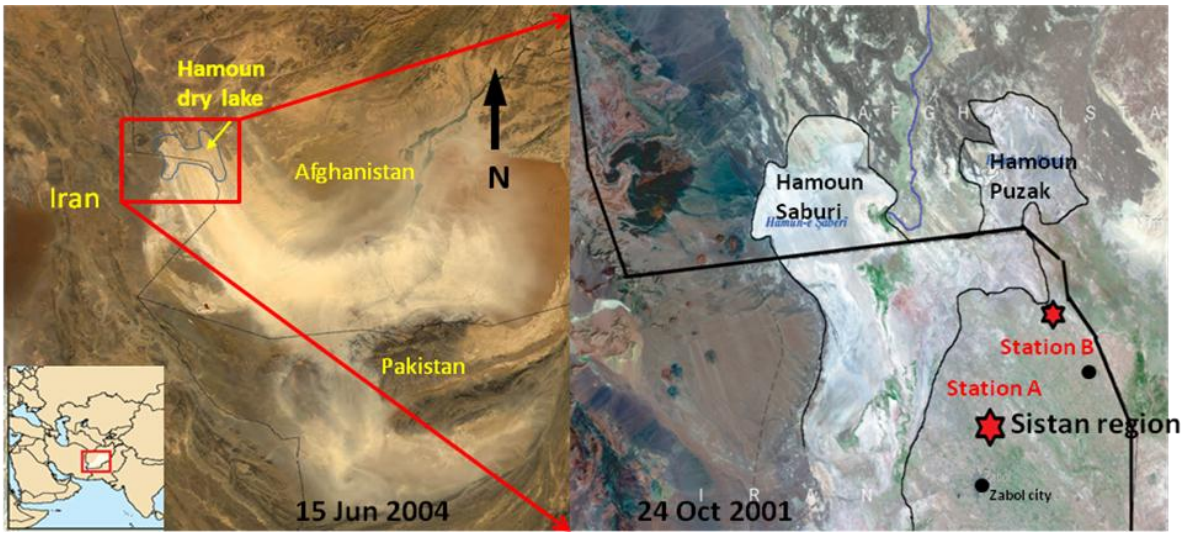

Figure 3.8: Locations of the dust loading measurement stations (stations A and B). The left image shows an intense dust storm that originated from the Hamoun basin on 15 June 2004 (Terra MODIS satellite image), while the right image zooms in on the Hamoun wetlands on 24 October 2004.

The dust sampler used in the campaign was developed by the Agricultural and Natural Research Center of Sistan, and is a modified version of the SUSTRA sampler (Janssen and Tetzlaff, 1991) and the SSDS sampler (Ekhtesasi *et al*., 2006; 2009). At the observation sites, the samplers collect airborne dust sediment. The traps were mounted on a stable bracket parallel to the wind direction. The samplers consist of a tube with a diameter of 12 cm. The sediment-laden air passes through a vertical 2.5 cm x 6 cm

sampler opening in the middle. Inside the sampler, air speed is reduced and the particles settle in a collection pan at the bottom, while the air discharges through an outlet with a U shape. After each measurement, the samplers were evacuated to make them ready for measuring the following dust events. The collected samples were oven dried at 105 ^{o}C for 24 hours, and then, dried samples were weighed using an electronic scale with 0.001 g precision in order to obtain total mass quantities at each sampling height and for each dust storm.

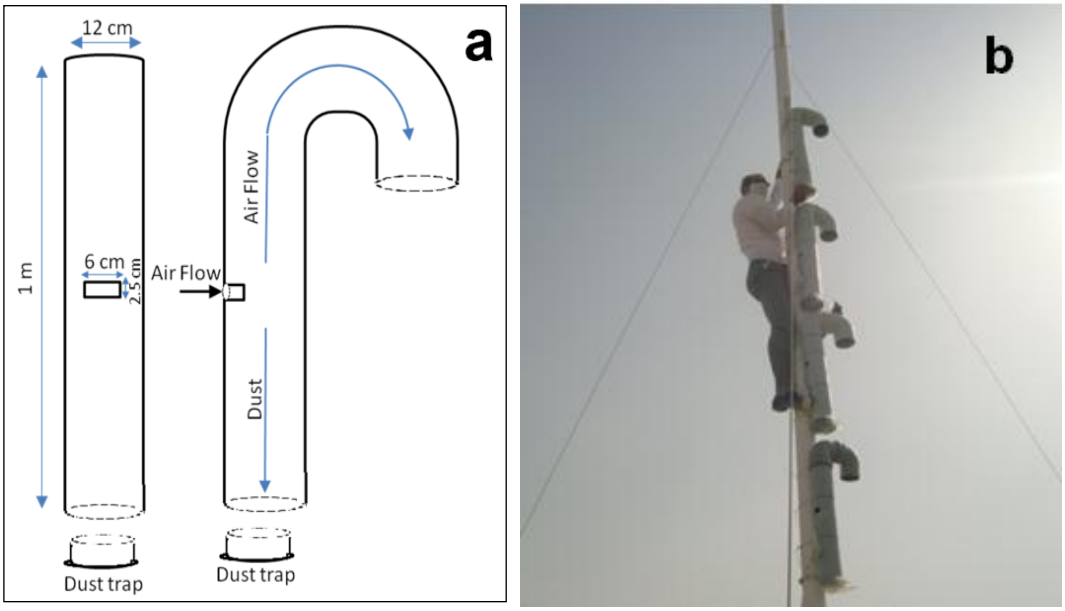

Figure 3.9: Schematic diagram of (a) the dust sampler system and (b) photo of the eight meters dust monitoring tower.

3.5.2 Particle-size analysis

The particle-size distribution of the collected samples was determined with a Malvern Mastersizer 2000 analyzer (Fig 3.10) with a measurement range of 0.02 to 2000 µm at Lanzhou University, China. The samples were pre-treated with 10 to 20 ml of 30% H_2O_2 to remove organic matter and then with 10 ml of 10% Hydrochloric acid (HCl) to remove carbonates. Then, about 2000 ml of de-ionized water was added and the sample solution was kept for about 24 h to rinse acidic ions. The residue sample was finally treated with 100 ml of 0.05 M $(NaPO_3)_6$ on an ultrasonic vibrator for 10 min to facilitate dispersion before grain-size analysis. The Mastersizer 2000 automatically yields the

median diameter and the percentages of the related size fractions of a sample with a relative error of less than 1%.

Figure 3.10: Measurement of dust particle-size using the Malvern Mastersizer 2000 analyzer (Lanzhou University, China).

3.6 Results and discussion

3.6.1 Dust loading measurements

Dust activity is a function of several parameters, such as topography, rainfall, soil moisture, surface winds, regional meteorology, boundary layer height and convective activity (Middleton and Goudie, 2001; Knippertz *et al*., 2009). The dust loading measured at the two stations close to the Hamoun basin for several dust events during the period August 2009 to July 2010 is plotted in Fig. 3.11. In the same graph, meteorological data from the Zabol station that give information about the duration of dust events (for the examined days as well as in the preceding or succeeding days) and daily mean and maximum wind speeds, are also plotted.

The results of the average dust loading measured at eight heights at station B and at four heights at station A reveals considerable variation, ranging from ~0.10 to ~2.5 kgm^{-2}. The average dust loadings for all the examined days were found to be 0.89 $kg.m^{-2}$ (station A) and 0.93 kgm^{-2} (station B), which do not exhibit a statistically significant difference. In general, the highest dust loading is observed for dust events occurring in summer, but

intense dust storms can also take place in winter, since the Hamoun basin is located in an active dust source region throughout the year.

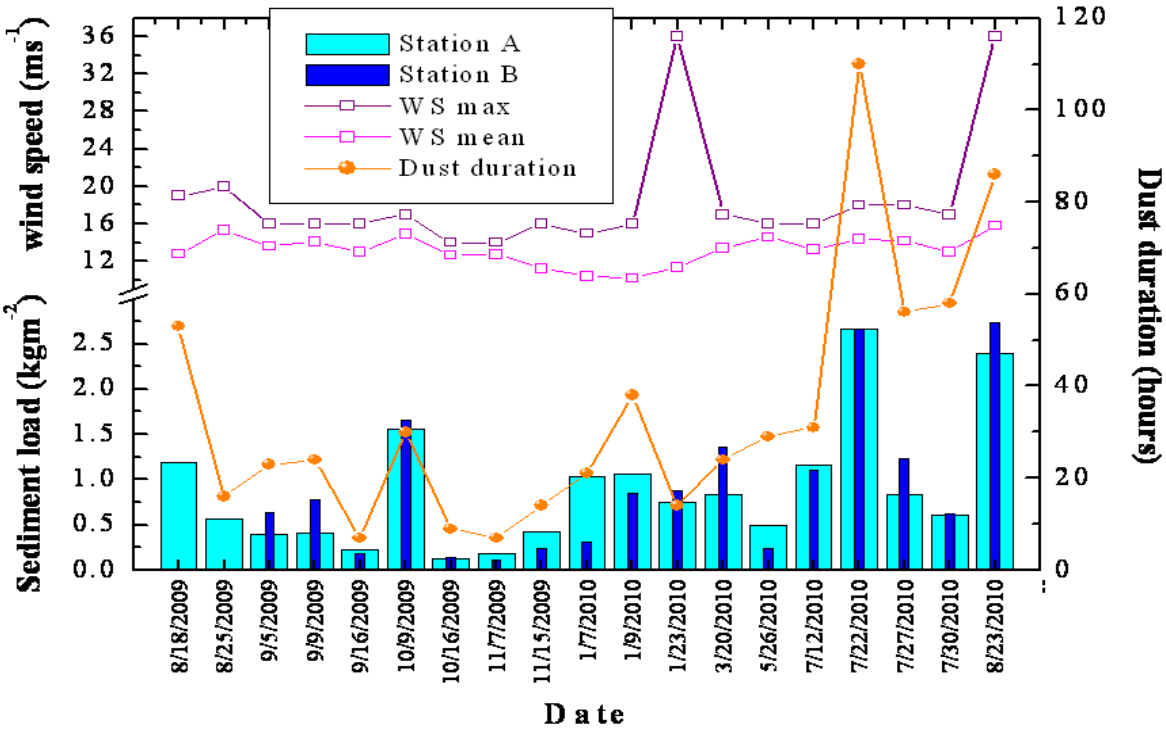

Figure 3.11: Average dust loading (kgm^{-2}) during various dust events in the Sistan region as measured at the 4m (station A) and 8m (station B) monitoring towers. The duration of dust events (hours), as well as the mean and maximum wind speeds on the dusty days were obtained from the Zabol meteorological station.

The dust loading is highly correlated with the duration of the dust storms, as shown from their correlation, with the linear regressions being statistically significant at the 0.99% confidence level (Fig. 3.12). Apart from the strong linke to the duration of dust storms, the dust loading at both stations also seems to have a dependence on the daily mean and maximum wind speeds (Figure not shown). However, this dependence was found to be more intense and statistically significant (at the 95% confidence level) at station B, which is located closer to the dust source, whereas for station A the correlation was not found to be statistically significant. This finding emphasizes the strong effect of the wind speed on dust erosion and transportation, as well as on dust loading, at least for areas close to dust sources. However, the results show that the main factor that controls the dust loading at both stations is the duration of the dust storms, and secondly the wind speed. The role of the wind might have been found to be more critical if measurements were taken at the sampler stations instead of using the meteorological data from Zabol. The total amount of dust loading represents large variation depending on intensity,

duration and particle size distribution for each dust event. The analysis showed that the total dust loading for the 19 events of measurements at station A is 16.9 kg.m^{-2} corresponding to 0.88 kg.m^{-2} per event, whereas at station B the measurements yielded 15.8 kg.m^{-2} (17 events), corresponding to 0.93 kg.m^{-2} per event. The larger dust loading at station B is attributed to the smaller distance from the source region.

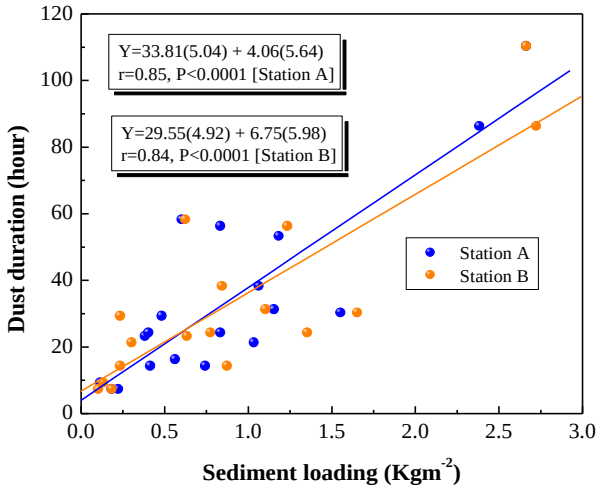

Figure 3.12: Correlation between dust loading measurements and duration of dust storm events for 19 days at station A and 17 days at station B.

Data on dust loading are available at only a few places around the world (e.g. Zhang, 1985; Offer and Goossens, 2001; Dong et al, 2010) and those presented here are the first for the Sistan region. Hence, obtaining measurements of horizontal dust flux will significantly increase our understanding of wind erosion and dust problems. Apart from the natural emissions of dust, Zender et al. (2004) identified two ways in which human activities can influence dust emissions: (a) by changes in land use, which alter the potential for dust emission, and (b) by perturbing local climate that, in turn, alters dust emissions.

Figure 3.13 illustrates the height variation in dust loading during the dust storms measured at station A (19 days, up to 4m in height) and station B (17 days, up to 8m in height). Contrasting height variations measured during intense dust storms occurred between the two stations, while similar variations correspond to moderate and low storm events. More specifically, the dust loading shows an increase (decrease) with height in station A (station B), revealing a difference in the dust transport mechanisms. This finding can be explained by considering the fact that station B is located closer to the Hamoun dust source region,

meaning that uplift and newly transported dust concentration is higher near the surface. On the other hand, at station A that is located about 20 km away, the dust loading presents larger values up to 3 m since the near-ground dust particles have already been deposited near the source, and as the distance increases so does the dust-plume height. The diurnal variability of the dust loading at the two stations (not presented) showed increased mass concentrations during daytime that can be explained by enhanced convection and turbulent mixing in a deepened boundary layer. Furthermore, the local winds are stronger during daytime due to thermal convection.

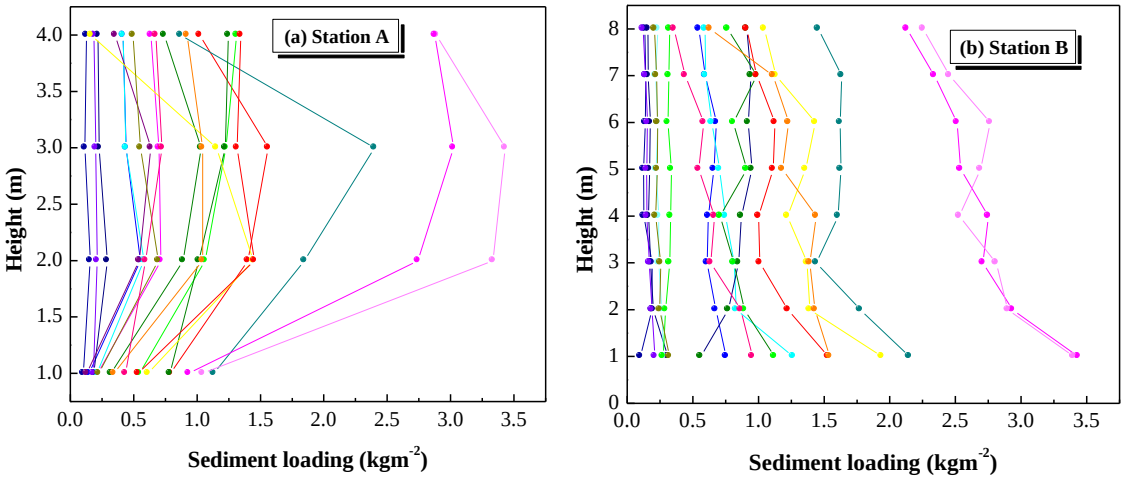

Figure 3.13: Height variation of dust loadings at stations A (a) and at station B (b) for several dust storm days. Green colors are loadings for winter, yellow for spring, red for summer and blue for autumn.

3.6.2 Dust grain-size distribution

Supplementary to the dust loading measurements, the dust grain-size distribution was analyzed for selected samples at stations A and B by means of a Malvern Mastersizer 2000 analyzer. More specifically, the dust grain size was analyzed for 31 samples collected on 12 days at four height levels at station A and for 44 samples corresponding to eight days (eight heights) at station B. The average grain sizes for the selected dust events at stations A and B are summarized in Tables 3.2 and 3.3, respectively. The d(0.5) corresponds to the median grain size (measured in μm) of the particle distribution, while the d(0.9) implies that 90% of the grain size of particles is below this value. The percentages of $PM_{2.5}$ and PM_{10} indicate the fraction of the particles that have diameters of below 2.5 and 10 μm, respectively.

The results in both Tables 3.1 and 3.22 show considerable variation in all grain-sized parameters, depending on the intensity of the dust storms as well as on other factors considering the soil materials. In general, dust storms that occurred during summer present larger grain sizes due to stronger durinal and seasonal winds (fig 2.8 and 2.9b). As a consequence, a smaller fraction of particles is below 10 and 2.5 µm. However, more measurements are needed for evaluating these results. The whole spectrum of grain-size measurements at both stations is analyzed in Figs. 3.14a and b. These figures show box charts for each parameter that allows for a direct comparison between the two stations.

Table 3.2: Variation in average grain size during different dust storms at station A.

Date	d (0.5)	d (0.9)	$PM_{2.5}$ (%)	PM_{10} (%)
19/08/2009	24.1	61.0	8	24
25/08/2009	19.9	56.0	11.0	30.0
05/09/2009	26.1	64.5	9.5	24.0
09/09/2009	28.2	73.8	10.5	26.0
16/09/2009	14.3	46.9	8	38
09/10/2009	23.8	63.4	10.3	27.5
15/11/2009	10.1	36.2	15.3	50.7
07/01/2010	14.8	56.0	11.7	40.8
09/01/2010	12.6	42.6	11.0	51.3
23/01/2010	13.5	45.0	11.0	41.5
08/07/2010	29.9	77.2	9.5	26.0
23/08/2010	31.5	80.6	8.0	20.8

Table 3.3: Variation in average grain size during different dust storms at station B.

Date	d (0.5)	d (0.9)	$PM_{2.5}$ (%)	PM_{10} (%)
05/09/2009	63	163	7	18
09/09/2009	55	149	7	17
16/09/2009	37	115	9	23
09/10/2009	61	159	7	19
16/10/2009	36	102	8	24
15/11/2009	32	96	9	25
07/01/2010	14	54	13	41
08/07/2010	49	147	9	22

The analysis of the dust's grain size reveals large differences between the two stations, especially for the d(0.9). For this parameter, the mean, median as well as the distribution

of the dust diameters are much higher at station B, exhibiting a mean value of 126.2±49.9 µm against that of 58.7±18.0 µm at station A.

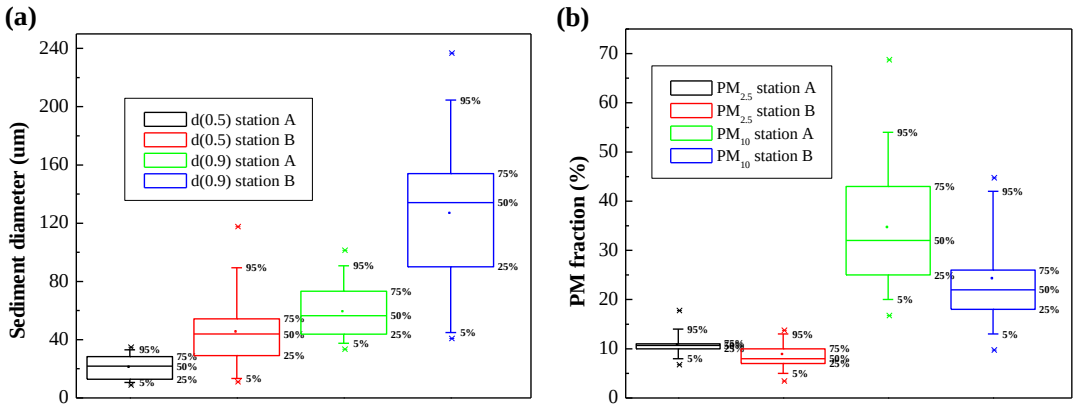

Figure 3.14: Chart boxes for (a) the dust diameters corresponding to d(0.5) and d(0.9) grain sizes and (b) for the fraction (%)lower than $PM_{2.5}$ and PM_{10} particles at both stations A and B.

In general, the median grain size (d0.5) distributions of settled desert dust in Sistan is in the range of ~10–118 µm for both stations, with larger particle sizes and distribution of values at station B (Fig. 3.14a). For example, 50% of the dust particles are below 20.5±8.1 µm at station A, while the same fraction is below 44.8±23.8 µm at station B, implying considerable shift to larger dust particles at station B. This is also clearly observed when plotting the frequency distribution of particle size (Fig. 3.15). In Fig 3.15 the maximum of the mean distribution is around 30 µm for station A, which increases to ~60 to 70 µm for station B. Note also the dominance of higher frequencies of dust particles above 100 µm at station B, while the difference between the distributions is rather low for the small particles. This is particularly valid for particles <2.5 µm, for which the results show fractions of 10.6±2.3% and 8.7±2.5% for stations A and B, respectively (Fig. 3.14b); much larger difference is shown for PM_{10}, which is in the order of 10%. Station B, which is closer to Hamoun, exhibits slightly higher dust loading and significantly higher fraction of large particles than that observed at station A, which is 20 km from B and further from Hamoun. This is indicative of significant spatio-temporal variation in dust sediment loadings and grain-size distribution, which emphasizes the necessity for more systematic measurements, even at some new locations around the Hamoun basin in order to obtain an improved understanding of dust characteristics around the Hamoun lakes.

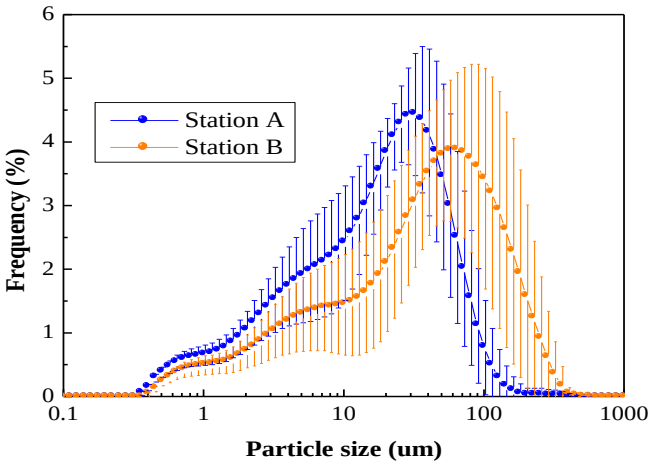

Figure 3.15: Average and standard deviation of the dust samples particle-size distribution at stations A and B.

Finally, Fig. 3.16 provides the mean height variation in grain size parameters at station B. The profiles show a considerable decrease with height, mainly in d(0.9) and secondarily in d(0.5), indicating a shifting of the size-distribution curves towards lower particle sizes. This suggests that the larger and heavier particles are found near the ground and that only the smaller particles are lifted to elevated heights meaning that they are more likely to be transported over large distances. As the particle size decreases, the height variability is gradually reduced, being neutral for $PM_{2.5}$, while for PM_{10} the percentage fraction profile indicates a larger probability for occurrence at higher levels.

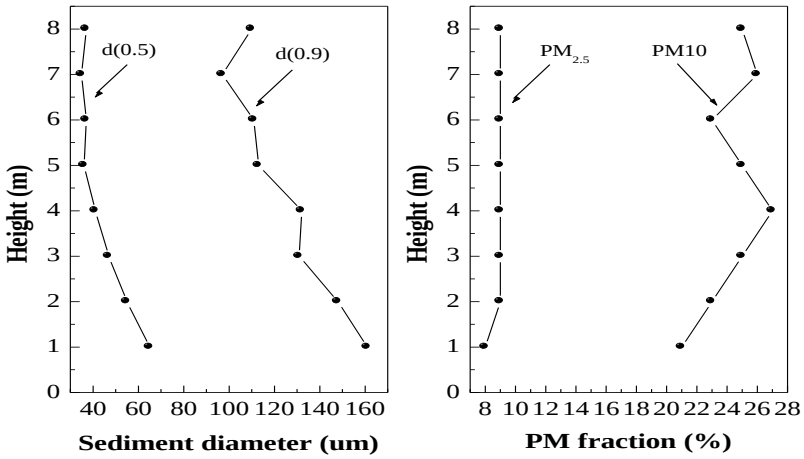

Figure 3.16: Average height variation of the grain size measured over eight days at station B for d(0.9) and (d0.5) (left panel) and $PM_{2.5}$ and PM_{10} (right panel).

3.7 Conclusions

This chapter provides analysis of the dust sediment loading and grain size distribution in the Sistan region, southeast Iran, based on first time measurements conducted at two locations that are situated close to the Hamoun basin. Hamoun is considered to be one of the most active dust source regions in Southwest Asia. Dust loading from the Hamoun basin has been found to have a significant contributing influence on the development of extreme dust storms, especially during the summer days. The influence firstly depend on the intensity and duration of dust storms, and secondarily, on the distance from the source region, the wind speed and altitude. The grain-size distribution of the dust loading was strongly influenced by the distance from the dust source, since grain sizes shifted to larger values towards station B that is closer to the Hamoun basin. Furthermore, the particle size distribution exhibited a shift towards lower values as the altitude increases, with this feature found to be more obvious amongst larger sized particles, while the frequency of particles below 2.5 μm seemed not to be affected by altitude. In general, the analysis revealed significant spatio-temporal variability of regional dust loading and characteristics. This finding necessitates more systematic observations at as many locations as possible around the Hamoun basin in order to improve the understanding of force dynamics, transport mechanisms as well as to quantify the dust amounts emitted from the Hamoun basin.